DOI: 10.1002/asia.200700025

Bioinspired Nanodevice Based on the Folic Acid/Titanium Dioxide System

Sylwia Gawęda, Grażyna Stochel, and Konrad Szaciłowski*[a]

Abstract: A new bioinspired nanomaterial has been obtained by chemisorption of folic acid onto nanocrystalline titanium dioxide. The organic chromophore is linked with the semiconductor surface via the glutamate chain and anchored with the carboxylate group. The geometry and electronic structure of the chromophore was studied in detail with DFT. Photoelectrochemical studies revealed photosensitization of the new material towards visible light. The photoelectrodes composed of the folic acid/titanium dioxide hybrid material generated photocurrent over a 300–600-nm window. Moreover, the direction of the photocurrent could be changed from anodic to cathodic and vice versa by application of the appropriate photoelectrode potential. Photoelectrochemical and spectroscopic studies allowed the elucidation of the mechanism of photocurrent switching. Photoelectrodes composed of folate-modified titanium dioxide may serve as a simple model of optoelectronic switches and may constitute the basis for molecular photoelectronic devices.

Keywords: folic acid · molecular devices · photochemistry · photosensitizer · titanium

Introduction

Molecules that comprise an electron donor and an electron acceptor with delocalized π-electron systems linked with an aliphatic bridge are of potential interest for molecular and organic electronics.[1–7] Devices based on organic materials should in principle combine the high performance of inorganic semiconductors with the processibility and low price of organic materials.[8] Molecules with low HOMO/LUMO gaps are of particular importance due to their ability to donate (from HOMO) or accept (in LUMO) an electron easily, which is the basic process in all organic electronic devices. Although any molecule can, in theory, act as an electron donor and an electron acceptor, only a few so-called electrochemically amphoteric compounds can do both within a readily accessible potential window to form stable redox states.[1]

The first single-molecule device, which works as a rectifier, was designed by Aviram and Ratner in 1974 (Scheme 1 a).[9] The molecule contains an electron-donor moiety (2,2′-bis(1,3-dithiolylidene), also known by the common name tetrathiafulvalene) and an electron acceptor (tetracyanoquinodimethane) bound together with a saturated [2.2.2]bicyclooctane linker. The delocalized bond systems of donor and acceptor should stabilize the ionized form of the molecule (D^+–σ–A^-) while the σ bridge decouples the molecular orbitals of the donor from those of the acceptor. In this way, HOMOs are localized mainly on the donor part of the molecule, and LUMOs on the acceptor part. When placed between two metallic contacts, the molecule should behave as a rectifier, that is, it transmits electrons only in one direction. The first molecular system experimentally proven to work as rectifiers according to the Aviram–Ratner principle was hexadecylquinolinium tricyanoquinodimethanide (Scheme 1 b).[10]

Similar molecular setups were used to mimic charge separation in photosynthesis and in organic photovoltaic devices.[11–19] In contrast to the previously discussed systems, these molecules must be equipped with efficient photonic

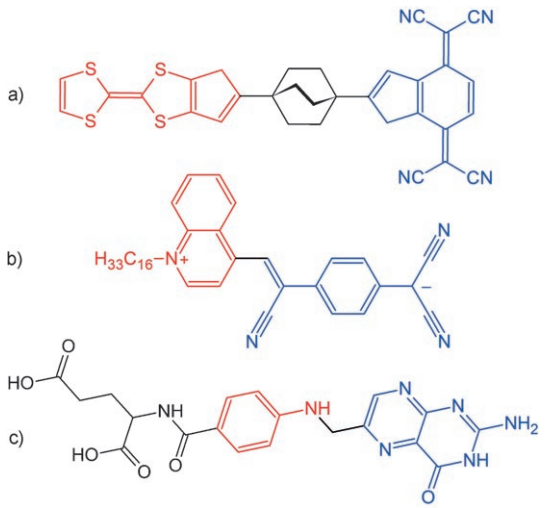

Scheme 1. Molecular structures of selected single-molecule electronic devices. a) The Aviram–Ratner "Gedankenmolekül".[9] b) Hexadecylquinolinium tricyanoquinodimethanide, the first experimentally proven molecular rectifier.[10] c) Folic acid. Electron-donor and electron-acceptor moieties are shown in red and blue, respectively.

[a] S. Gawęda, Prof. Dr. G. Stochel, Dr. K. Szaciłowski
Centrum Nanochemii Nieorganicznej
Wydział Chemii
Uniwersytet Jagielloński
ul. Romana Ingardena 3, 30-060 Kraków (Poland)
Fax: (+48) 12-634-0515
E-mail: szacilow@chemia.uj.edu.pl

antennae to harvest energy utilized for charge separation. In the most cases, these antennae comprise porphyrins or related chromophores that serve simultaneously as the electron donors, whereas fullerene moieties serve as the electron acceptors.[20] The charge-separated state resulting from photoinduced electron transfer can drive various redox processes in solution or inject electrons to the conducting support, which in turn results in photocurrent generation.

In general, the electrical and photoelectrical properties of covalently linked but electronically decoupled donor–acceptor systems resemble those of the classical, semiconductor-based diode (rectifier). A diode is understood herein as a device composed of two layers of semiconducting material, *p*-type and *n*-type, containing acceptor and donor dopant atoms, respectively. In molecular devices, the diodelike structure is obtained by linking electron-rich (*n*-type) and electron-poor (*p*-type) organic moieties.

Recent advances in photovoltaics[19,21–24] and semiconducting nanodevices[25–30] result from developments in the photochemistry and photophysics of bulk- and surface-modified wide-band-gap semiconductors. The surface complex formed by chemisorption of various transition-metal complexes on the surfaces of mesoporous and nanocrystalline wide-band-gap semiconductors usually plays the role of light-harvesting antenna, whereas the semiconducting structure acts as a charge-separation device and provides a mechanical support for the photosensitizer.[21,31,32] Various hybrid systems based on nanoparticles "decorated" with biomolecules are in the limelight in chemistry, biotechnology, and materials science. These systems can be used as sensors, markers, (photo- or electro-) catalysts, and biomimetic models of complex biological systems.[33–39]

The inspiration for light-harvesting molecules and antenna systems capable of titania photosensitization comes from various biosystems[20] and may include inspiration by function and structure. Both approaches may lead to biomimetic systems, which imitate natural systems, or fully artificial systems that, on the other hand, utilize natural biomolecules. The present results fall into the second category.

There are numerous trials of the construction of photosensitized solar cells that are based on biomolecules and supramolecular bioinspired systems, for instance, chlorophylls,[40,41] porphyrins,[42–46] phthalocyanines,[47] and other natural or biomimetic dyes.[48–52] In every case, the redox-active molecules supply electrons from their excited states. Therefore, the redox properties of an excited photosensitizer must correlate with the potential of the conduction-band edge of the applied semiconductor.

Among various redox-active chromophores, folic acid (FA) has a structure that most closely resembles that of the Aviram–Ratner "Gedankenmolekül". It is an intramolecular donor–acceptor system assembled via the σ bridge (Scheme 1c). Folic acid belongs to the group of pterin cofactors. These compounds are derived from 2-aminopteridin-4(1*H*)-one (pterin). They participate in various relevant physiological functions that are usually associated with electron-transfer processes[53,54] or light harvesting.[55,56] Folic acid derivatives can behave as light-harvesting antennae in the DNA repair enzymes photolyases.[55,57,58] Therefore, folic acid is a promising redox-active chromophore for the modification of wide-band-gap semiconductors. Moreover, it is equipped with anchoring groups suitable for its facile immobilization on semiconducting surfaces,[59,60] and its optical properties make it suitable for photosensitization of wide-band-gap semiconductors such as TiO_2. This paper presents electrochemical, spectroscopic, and photoelectrochemical investigations into semiconducting devices based on titanium dioxide modified with folic acid.

Abstract in Polish: Poprzez chemisorpcję kwasu foliowego na powierzchni dwutlenku tytanu otrzymano nowe nanomateriały bioinspirowane. Chromofor organiczny jest połączony kowalencyjnie z powierzchnią półprzewodnika za pośrednictwem grup karboksylanowych łańcucha glutaminianowego. Geometria i struktura elektronowa chromofora zostały dokładnie określone za pomocą obliczeń techniką DFT. Badania fotoelektrochemiczne wykazały silną fotosensybilizację półprzewodnika na światło widzialne. Fotoelektrody zbudowane z dwutlenku tytanu modyfikowanego kwasem foliowym generują fotoprądy w zakresie 300-600 nm. Ponadto stwierdzono, że kierunek fotoprądu (anodowy lub katodowy) może być zmieniony poprzez zmianę polaryzacji podłoża przewodzącego. Pomiary fotoelektrochemiczne uzupełnione badaniami spektroskopowymi pozwalają na określenie machenizmu przełączenia fotoprądu. Fotoelektrody zbudowane z materiału hybrydowego mogą pozwolić naudowę przełączników optoelektronicznych i bardziej złożonych układów logicznych.

Results and Discussion

Molecular and Electronic Structure of Folic Acid

The folic acid molecule comprises three molecular units: pterine, aminobenzoic acid, and glutaminic acid. According to DFT calculations, the two aromatic systems are almost coplanar (tilt angle $\approx 1°$) and are separated by one sp^3-hybridized carbon atom. The glutamate side chain is localized on the same geometrical plane as the rings (Figure 1).

The donor–acceptor character of the folic acid molecule can be seen in the charge distribution in the ground and first excited states. In the ground state, charge distribution is quite uniform, but the aminobenzoate moiety bears significant negative charge, whereas the pterine moiety is positively charged (Figure 1a). Upon excitation, the electric charge on the pterine moiety decreased but increased on aminobenzoate (Figure 1b), clearly indicating charge transfer from aminobenzoate to pterine.

Further support of the donor–acceptor architecture of folic acid comes from molecular-orbital calculations (Figure 2). The HOMO and LUMO orbitals of the donor and acceptor parts form two independent orbital systems,

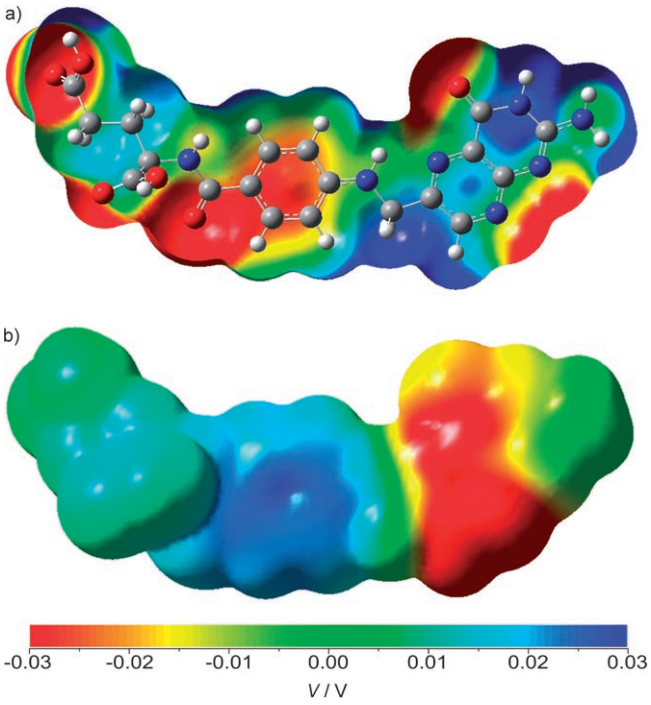

Figure 1. a) Molecular structure and electrostatic potential map superimposed onto the electron density of the folic acid molecule in the ground state. b) Change in electrostatic potential upon excitation to the first excited state as calculated at the B3PW91/6-311++G(d,p) level of theory with tight convergence criteria.

Electrochemical and Photophysical Properties of Folic Acid

Folic acid can adopt up to two electrons on the pterine moiety, and the *p*-aminobenzoate moiety serves as an electron donor. Quasireversible one-electron reduction of folic acid in *N*,*N*-dimethylformamide (DMF) proceeded at −0.82 V versus Ag/AgCl. Oxidation of folic acid took place at +1.16 V versus Ag/AgCl (Figure 3a). The difference between these two potentials constitutes a rough estimate of the HOMO–LUMO gap, as the reduction process is localized at the LUMO orbital and oxidation at the HOMO. The

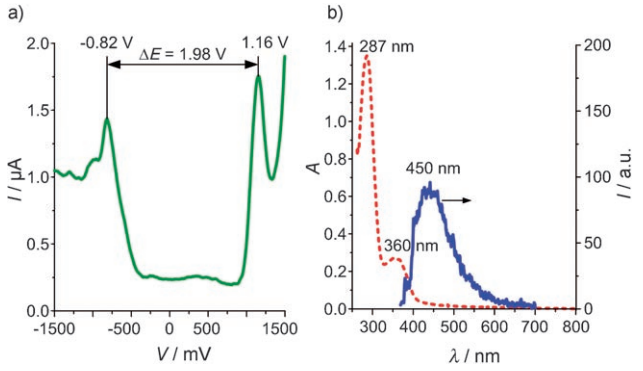

Figure 3. a) Differential pulse voltammogram recorded at the Pt disc electrode in a solution of folic acid in DMF. b) Absorption (red) and fluorescence (blue) spectra of folic acid in DMF. Excitation wavelength = 360 nm.

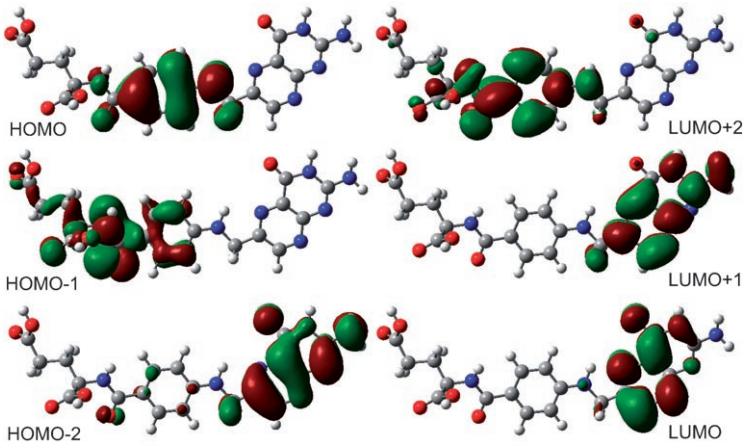

Figure 2. Molecular orbitals of the folic acid molecule in the ground state as calculated at the B3PW91/6-311++G(d,p) level of theory.

and no delocalized molecular orbital overlapping both aromatic systems was found near the HOMO–LUMO frontier. This electronic configuration is well-suited for diodelike behavior, as the donor and acceptor molecular orbitals are well-separated in space and energy domains due to the σ bridge.

electrochemically evaluated HOMO–LUMO gap (the difference between the oxidation and reduction potentials) amounted to 1.98 eV.

The absorption spectrum of folic acid in DMF shows two strong bands at 287 and 360 nm (Figure 3b). Time-dependent (TD)-DFT calculations indicate that the lower-energy band corresponds to the HOMO→LUMO transition, whereas the band at 287 nm corresponds to the HOMO→LUMO+1 transition. The fluorescence spectrum of folic acid in DMF shows one peak at 460 nm. The excitation spectrum recorded at this emission wavelength exhibits a maximum at 360 nm, so the luminescent excited state results from HOMO→LUMO excitation. This data led to an estimate of the HOMO–LUMO gap of 2.70 eV. According to DFT calculations, the difference between the HOMO and LUMO energies is 1.95 eV, which is in perfect agreement with the electrochemical data. The energy of the lowest-energy transition was calculated by using TD-DFT to be 2.34 eV, which is close to the experimental value. The discrepancy between the spectroscopic and the electrochemical band-gap estimate is well-reflected in the DFT-calculated values. This discrepancy originates from the large reorganization energy associated with the HOMO→LUMO transition due to the generation of a large dipole moment resulting from charge separation be-

tween aminobenzoate and pterine moieties. The large reorganization energy[61] can be also deduced from the very large Stokes shift ($\approx$0.5 eV).

Interaction of Folic Acid with Titanium Dioxide

Impregnation of nanocrystalline titanium dioxide with a solution of folic acid in DMF resulted in a yellow material. Chemisorption of folic acid onto the titanium dioxide surface is relatively strong; even prolonged contact with water, ethyl alcohol, acetic acid, or DMF did not alter the optical properties of the material and the solvent. Slow desorption of folic acid from the TiO_2 surface was observed in aqueous solutions of high pH. This observation indicates that the chemisorption of folic acid at TiO_2 involves the carboxylate groups of the glutamate side chain, as can be expected from the strong affinity of titanium dioxide towards COO^- groups.[59]

The electronic spectrum of folic acid in the solid state differs significantly from the solution spectrum. In the solid phase, an additional transition was observed at 450 nm. This new absorption may have originated from intermolecular transitions between folic acid molecules packed in the molecular crystal. The planarity of the molecule enables efficient π–π stacking,[62–64] while the presence of proton donors and acceptors within the pterine ring gives the possibility of formation of a whole series of hydrogen bonds.[63–66] These intermolecular interactions result in a semiconductor-like band structure, which in turn results in the low-energy absorption band centered at 450 nm. The formation of the band structure in molecular crystals of folic acid can be substantiated by photoelectrochemical measurements. Irradiation of commercially available crystalline folic acid deposited onto an indium tin oxide (ITO) electrode resulted in the generation of anodic photocurrent. Its action spectrum over 300–600 nm resembles the diffuse reflectance spectrum of folic acid. Interestingly, the maximal photocurrent value was recorded at 360 nm, which perfectly matches the low-energy electronic transition within folic acid (HOMO→LUMO). Irradiation within the low-energy band observed at around 450 nm also resulted in photocurrent generation. This indicates that solid folic acid behaves like an *n*-type semiconductor, which is in agreement with its donor–acceptor structure.

The diffuse reflectance spectrum of folate-modified titanium dioxide shows spectral features characteristic of neat folic acid in DMF: an intense transition at 290 nm and a much weaker one at 375 nm. Almost-identical absorption bands were also found in the diffuse reflectance spectrum of solid folic acid. No separated band at around 450 nm was seen, which indicates a lack of significant interaction between individual molecules of folic acid. The low-energy tail of the spectrum over 400–550 nm must have originated from charge-transfer interactions between the semiconducting support and the organic chromophore.[67] This interaction may involve formation of hydrogen bonds between the pterine moiety and the hydroxy groups of the TiO_2 surface. The identity of this transition was confirmed spectroscopically in the system containing folic acid and titanium dioxide quantum dots. Addition of TiO_2 nanoparticles to a solution of folic acid in DMF resulted in new absorption bands at 330 and 410 nm (Figure 4, inset). The latter band tails down to 550 nm, which is consistent with observations for folic acid modified titanium dioxide.

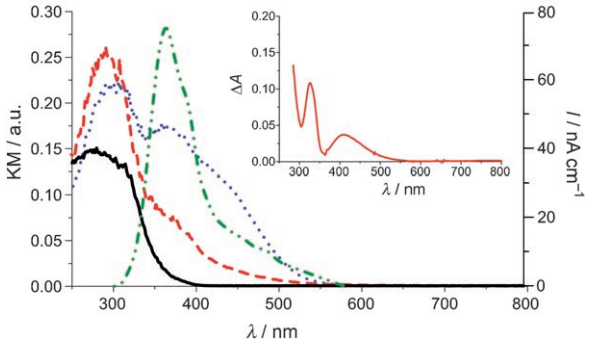

Figure 4. Diffuse reflectance spectra of titanium dioxide (black), folic acid (blue), and folate-modified titania (red), and photocurrent action spectrum recorded for folic acid deposited on ITO electrode (green). Inset: differential absorption spectrum of TiO_2 nanoparticles in a solution of folic acid in DMF.

Photoelectrochemical Properties of FA/TiO_2

The interaction between the photosensitizer and the semiconducting support should influence the energy (or redox potentials) of the conduction- and valence-band edges (CBEs and VBEs, respectively). These data can be obtained from measurements of the quasi-Fermi level[68,69] (i.e., the Fermi level potential measured for a semiconducting material under irradiation, E_{qF}), which, together with the spectral characteristics of the synthesized materials, allow the determination of the redox properties of the excited semiconducting materials. The modified method of quasi-Fermi level determination[68] described by Roy et al.[69] was applied. This method is based on the pH dependency of the potentials of the VBEs and CBEs of the semiconductor particles. In the case of titanium dioxide, with increasing pH a cathodic shift of E_{qF} by 59 mV per pH unit was reported[68,69] ($k = -0.059$ V). In combination with a pH-independent reversible redox pair (e.g., a compound from the group of viologens), the electrons from the conduction band of the irradiated semiconductor can either reduce the redox couple or not, depending on the pH value and relative potentials (Figure 5). At pH values lower than pH_0 (i.e., the pH at which the potential lines cross), the photoinduced reduction of the redox couple does not take place. This process is, however, possible in more-basic media. Therefore, the measurement of E_{qF} assists in the determination of the pH_0 value.

The measured pH_0 value (Figure 6), that is, the pH at which the quasi-Fermi level potential equilibrates with the redox potential of the methylviologen$^{+\cdot}$/methylviologen^{2+}

CHEMISTRY
AN ASIAN JOURNAL

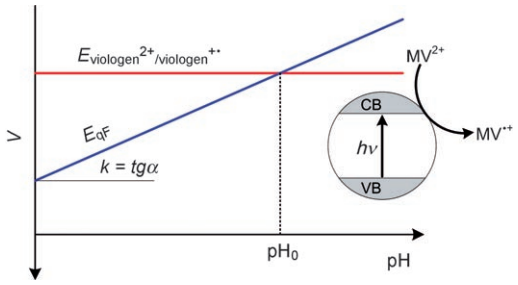

Figure 5. Principle of the measurement of quasi-Fermi level potential.

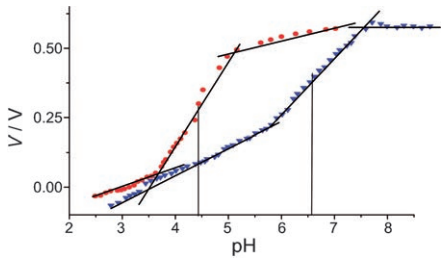

Figure 6. Determination of pH_0 for neat (red) and FA-modified titanium dioxide (blue).

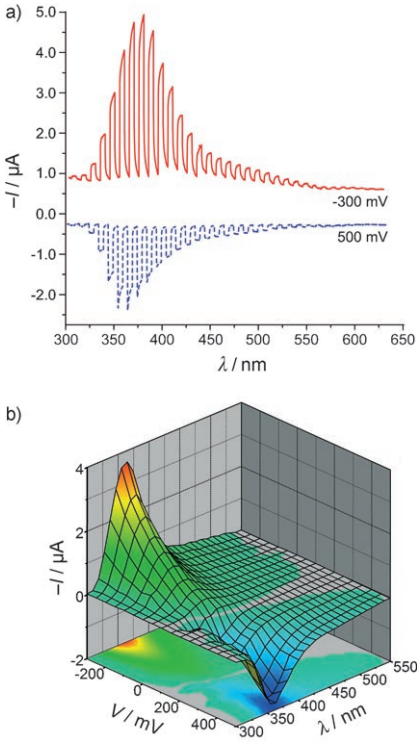

Figure 7. a) Photocurrent profiles recorded during pulsed irradiation of FA/TiO_2 with positive (red) and negative (blue) polarization of the photoelectrode. b) Action spectra recorded at FA/TiO_2 photoelectrodes as a function of electrode potential in oxygen-saturated electrolyte.

couple, enables the calculation of the quasi-Fermi level potentials.

The method of Roy yields pH_0 values for TiO_2 and folic acid modified TiO_2 of 4.45 and 6.54, respectively. This allows the calculation of CBE potentials according to [Eq. (1)]:

$$E_{CBE}(pH) = E^{\circ} + k \cdot (pH_0 - pH) \quad (1)$$

in which $E_{CBE}(pH)$ is the CBE potential at a given pH, $E°$ is the redox potential of the reference redox couple, and k is the factor of 59 mV resulting from the Nernst equation. In neutral solution (pH 7), the CBE potential is −0.58 and −0.47 V for neat and folate-modified TiO_2, respectively. These data are consistent with previous results reported for chloroplatinate-[70,71] and cyanoferrate-modified[28,72] titanium dioxide. Assuming that the TiO_2 band gap is not affected by modification, calculation of the upper-edge valence-band potential is also possible and gives 2.47 and 2.58 V for neat and modified TiO_2, respectively. This shift is consistent with previous observations. Substitution of the surface OH groups with anionic species resulted in the VB and CB shifting towards more-positive potentials owing to electrostatic repulsion of electrons within the semiconductor structure with the negatively charged surface species.[70,72]

Irradiation of photoelectrodes prepared from FA/TiO_2 resulted in the generation of photocurrent, the characteristics of which is very different from that recorded for neat titanium dioxide. In air-equilibrated and oxygen-saturated solutions, the photoelectrode generated anodic photocurrents only at positive polarization (Figure 7a). Negative polarization of the photoelectrode resulted in reversal of the direction of photocurrent. Interestingly, the cathodic photocurrent intensities are higher than the anodic ones. Such anomalous behavior was previously observed for cyanoferrate-modified TiO_2 photoelectrodes and is called the PEPS effect (photoelectrochemical photocurrent switching).[28,73,74]

To characterize the photocurrent-switching processes, a 3D photocurrent action spectrum was recorded over a wide potential range (Figure 7b). Both cathodic and anodic photocurrents were generated within the visible part of the spectrum (300–550 nm), and the photocurrent switching was very sharp in contrast to cyanoferrate-modified TiO_2.[73,74] In the absence of oxygen, the photoelectrochemical properties of the FA/TiO_2 photoelectrodes are very different. At positive potentials, the behavior of the electrode is much the same: anodic photocurrents of moderate intensity were observed at 300–550 nm. At 200 mV the photosensitization disappeared, and only weak anodic photocurrents characteristic of neat titanium dioxide photoelectrodes were observed.

Furthermore, within the absorption range of neat TiO_2 (300–420 nm), the photocurrent intensities are much higher than in the photosensitized region (420–550 nm). This indicates the occurrence of two parallel photophysical processes: excitation of the inner parts of titanium dioxide and excitation of the surface of the nanocrystals. Elucidation of the mechanism of photocurrent generation requires analysis of

the energy levels of the FA/TiO_2 system in aqueous electrolyte.

Redox potentials of folic acid in the first excited state can be calculated from the ground-state redox potentials and the energy of the lowest excited state as follows (Equations (2) and (3), Figure 8):[75–78]

$$E_{1/2}(^*D/D^+) = E_{1/2}(D/D^+) - E_{0,0} \quad (2)$$

$$E_{1/2}(^*A/A^-) = E_{1/2}(A/A^-) - E_{0,0} \quad (3)$$

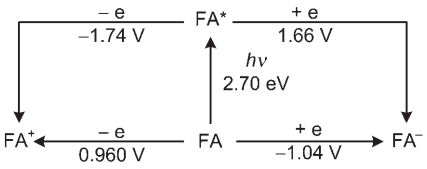

Figure 8. Latimer-type diagram of oxidation and reduction potentials of the ground and lowest excited states of the folic acid molecule.

These data, together with previously determined semiconductor-band-gap and CBE potentials, are the basis for the energy diagram of the studied system. Clearly, folic acid in the lowest excited state is a very good electron donor (−1.74 V vs. normal hydrogen electrode (NHE)) and a very good electron acceptor (1.66 V). The excited state of folic acid is a much stronger reducing agent than the conduction-band electrons (−0.58 V). On the other hand, holes in the valence band are the strongest oxidants in the system (2.47 V) (Figure 9).

Excitation of the electrode within the absorption range of the semiconductor at positive polarization of the photoelectrode resulted in a photoanodic response according to the generally accepted mechanism (Figure 10a). An electron is promoted to the conduction band of the semiconductor and is subsequently transferred to the conducting electrode. The hole in the valence band is in turn neutralized by the electron from oxidation of the solvent molecule. Excitation within the FA absorption results in similar processes. The excited state of folic acid, which is a good electron donor, can inject an electron into the electrode, either directly or via the conduction band of the semiconducting particle. The FA* state cannot oxidize free water molecules directly, but hydrogen bonding of the pterine moiety with solvent molecules may shift the oxidation potential significantly. This interaction may result in coupled proton and electron transfer and, thus, facilitate water oxidation. This process can occur only with positive polarization of the electrode; it is otherwise prevented by the electrostatic barrier (Figure 10b).

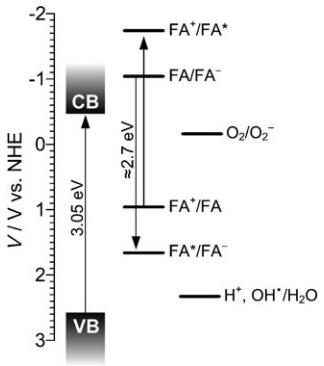

Figure 9. Redox potentials of titanium dioxide VB and CB relative to those of the ground and lowest excited state of folic acid, water, and molecular oxygen at pH 7.[79] Vertical arrows indicate possible excitation of the inner part of the semiconductor particle (3.05 eV) and surface-immobilized folic acid (2.7 eV).

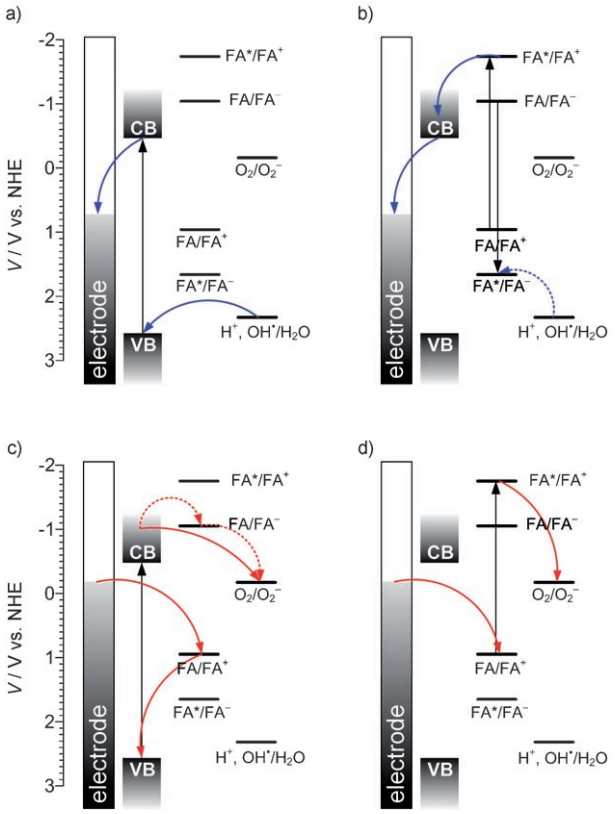

Figure 10. Mechanism of photocurrent generation (the PEPS effect). Anodic photocurrent is generated at positive potentials upon excitation of a) the inner part of the TiO_2 particle and b) surface folic acid, whereas cathodic photocurrents are generated at negative potentials upon excitation of c) TiO_2 or d) folic acid. The shaded vertical bars indicate the photoelectrode potential.

With negative polarization of the photoelectrode, a cathodic photocurrent was observed, but only in the presence of an efficient electron acceptor, for example, molecular oxygen. Neat titanium dioxide photoelectrodes yielded cathodic photocurrents only upon doping,[80] surface modification,[72–74] or at high pH.[81] The potential difference between the electrons in the conduction band and the O_2^-/O_2 couple is small, so there is not much thermodynamic driving force for this reaction. Moreover, interfacial electron transfer between the titanium dioxide surface and molecular oxygen strongly depends on surface adsorption of O_2. On the surface of neat TiO_2, recombination dominates over

electron transfer with dissolved oxygen, whereas on more-hydrophobic surfaces processes that involve molecular oxygen are much more effective.[82] The presence of folic acid on the surface thus facilitates oxygen reduction due to increased hydrophobicity and the electron-transfer properties of FA. The hole within the valence band can be easily neutralized by an electron from the folic acid molecule, which subsequently is reduced electrochemically. This process hampers the electron–hole recombination; the only possibility of an electron in the conduction band is to reduce the oxygen molecule either directly or via the electron-transfer process involving the folic acid molecule (Figure 10c). The excited state of folic acid is a much stronger electron donor (−1.74 V), so it can very easily reduce oxygen, and the folic acid cation radical thus generated can be easily reduced electrochemically (Figure 10d). The strongly reducing state can be generated either directly (by excitation of surface FA molecules) or indirectly via energy transfer from the excited semiconducting support. The latter process yields even higher photocurrent intensities than the former, owing to high absorptivity of titanium dioxide compared with the monomolecular layer of folic acid.

The photocurrent-switching mechanism is based mainly on the electron-donor and electron-acceptor properties of folic acid. Depending on photoelectrode potential, it may contribute to generation of anodic and cathodic photocurrent, which is a unique feature among photosensitizers.

Conclusions

The hybrid material obtained by immobilization of folic acid on the surface of nanocrystalline titanium dioxide has interesting photoelectrochemical properties. It exhibits pronounced photosensitization towards visible light. Photoelectrodes built from FA/TiO_2 generate photocurrent over a 300–550-nm window. The polarity of the photocurrent can be changed through changes in the photoelectrode potential. The mechanism of this process is described in terms of photoinduced electron transfer involving both folic acid molecule and titanium dioxide support. Folic acid acts here as an electron buffer, donating or accepting electrons if necessary, depending on the photoelectrode potential.

The photocurrent switching observed here is closely related to the PEPS effect. In contrast to other switchable photoelectrochemical systems,[28,29,72–74] the photocurrent direction does not depend on the wavelength of incident light. Therefore, this system is less useful as an optoelectronic logic device, but can be used as a demultiplexer.[72] It can also be used as an oxygen sensor, because the switching to the cathodic mode relies on the presence of a molecular acceptor or other accessible electron acceptor. As folic acid can form a series of hydrogen bonds with a wide variety of substrates, the FA/TiO_2 system can be a platform for various photoelectrochemical sensors. Owing to their catalytic activity towards the photoreduction of molecular oxygen, folic acid/titanium dioxide photoelectrodes may also be a good starting point for photofuel cells, which utilize solar energy for catalytic oxidation of fuel and generation of electric current.

The FA/TiO_2 materials generate photocurrent on irradiation at 300–550 nm, but the photocurrent direction depends on the photoelectrode potential. Switching of the photocurrent polarity is observed at 100 mV versus Ag/AgCl. At potentials higher than the switching potential range, the electrodes generate anodic photocurrent, whereas at lower potentials cathodic photocurrents are observed. One can assign the logic values of "0" and "1" to the negative and the positive polarization of the photoelectrode, respectively. The switching characteristics allow it to be used as an optoelectronic two-channel demultiplexer (data selector). This device collects information in the form of light pulses and converts it into photocurrent pulses. Furthermore, the sign (direction) of photocurrent pulses depends on the photoelectrode potential. In other words, information in the form of photocurrent pulses can be directed into two output channels: cathodic and anodic. An electronic equivalent of this logic device is composed of two AND and a NOT logic gates (Table 1, Figure 11). The input data signal (light pulses) is applied to one input of both AND gates, while control signal goes to one AND gate directly and to the other via an inverter. In this configuration, one of the AND gates is in the ON state and the other is OFF (Table 1).

Table 1. Truth table for the two-channel demultiplexer presented in Figure 11.

Data	Control	Anodic output	Cathodic output
0	0	0	0
1	0	0	1
0	1	0	0
1	1	1	0

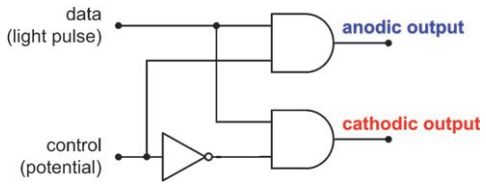

Figure 11. Electronic-equivalent circuit of surface-modified-titania photoelectrode working as a two-channel optoelectronic demultiplexer.

Thus, a signal applied to the data input is always transmitted by one of the AND gates and directed into one of the output channels. It is easy to imagine an application of similar systems in telecommunications. Nowadays information transmitted through optical fibers must be converted into electric signals and directed to the destination points. Therefore, the FA/TiO_2 system can serve as a simple two-channel demultiplexer. This is an interesting example of a simple chemical system working like a complex electronic circuit consisting of three logic elements.

The above examples show that nanocrystalline titanium dioxide modified with folic acid is a promising material for optoelectronics. Although very simple from the chemical point of view, it offers complex switching patterns as a result of its rich photoelectrochemistry. The most-interesting feature of this material consists of the complexity of electronic functions (Figure 11) contrasted with very simple morphology: Unstructured deposits of nanocrystalline powders show properties equivalent to complex circuits. Related materials may open a new field of nanoelectronics: rather than employing complex circuitry, designing a proper unstructured material of desired performance may be good enough.

Experimental Section

Materials

TiO_2 (Degussa P25, ≈70% anatase, 30% rutile; 50 $m^2 g^{-1}$) was used to prepare the porous electrodes. All other chemicals were supplied by Fluka and used as received. A small amount of folic acid was dissolved in hot (80 °C) DMF to yield a saturated solution. This was subsequently mixed with an equal volume of cold water, and the mixture was filtered to remove all the solids. A small sample of TiO_2 powder was suspended in the resulting solution of folic acid and stirred for 5 min. The modified TiO_2 was removed by centrifugation and washed five times with DMF and then five times with distilled water. Upon drying in air, folate-modified TiO_2 was obtained as a yellow powder. The ITO-coated glass slides (≈2 cm^2, Aldrich) were etched for at least 12 h in 15% NaOH, washed with distilled water, and air-dried. The semiconductor-modified nanopowder was suspended in distilled water, ultrasonicated, and cast onto the cleaned surface of the ITO-coated glass slides. After drying in hot air, copper wire was attached to the ITO surface with silver glue, and the whole junction area was protected with water-resistant self-adhesive insulation tape. Titanium dioxide nanoparticles were synthesized from hydrolyzed isopropyl orthotitanate. A mixture prepared from titanate ester (2.5 cm^3) and isopropyl alcohol (45 cm^3) was added dropwise to dilute nitric acid (450 cm^3, pH 1) over 1 h at 1 °C. The whitish colloidal solution was stirred overnight in an ice bath to yield a clear solution of TiO_2 nanoparticles.

Instrumentation

Absorption spectra were recorded on an HP 8453 (Hewlett–Packard) diode-array spectrophotometer. Fluorescence and excitation spectra were recorded on an LS45 (Perkin–Elmer) instrument. The typical three-electrode setup was employed for photoelectrochemical measurements. The electrolyte solution was 0.1 M KNO_3, which was kept in equilibrium with air or purged with argon for at least 15 min prior to measurement. Platinum and Ag/AgCl were used as auxiliary and reference electrodes, respectively. A 150-W XBO lamp (Osram) equipped with water-cooled housing and an LPS 200 power supply (Photon Technology International) was used for irradiation. The working electrodes were irradiated from the rear (through the ITO glass) to minimize the impact of the thickness of the semiconductor layer on the photocurrent. An automatically controlled monochromator and a shutter were applied to choose the appropriate energy of radiation. Dark electrochemical measurements were performed with platinum disc electrodes. The electrochemical measurements (CV, CV + chopped light, photocurrent action spectra) were controlled by BAS 50W (Bioanalytical Systems) or M161 (MTM) electrochemical analyzers. Cyclic voltammograms were recorded with a scan rate of 25 mV s^{-1}, and differential pulse voltammograms were recorded with the following parameters: scan rate 20 mV s^{-1}, pulse amplitude 50 mV, pulse width 50 ms, sample width 17 ms, pulse period 200 ms. Photocurrent action spectra were recorded under potentiostatic conditions and automatically corrected for dark currents. They were not corrected for light intensity. Diffuse reflectance spectra were recorded on a Shimadzu UVPC-2101 spectrophotometer equipped with an integrating sphere of 5-cm diameter. Barium sulfate was used as a reference material. CBE potentials were determined by using a modified Roy procedure.[69] A sample of semiconductor powder (40 mg) was suspended in aqueous potassium nitrate (70 cm^3, 0.1 M) and sonicated for 5 min. Methylviologen bis(hexafluorophosphate) (30 mg) was added, and resulting mixture was acidified with concentrated perchloric acid (1 cm^3). The suspension was placed in a rectangular glass vessel equipped with a combined-pH electrode, a platinum-foil electrode (area 2.5 cm^2), and a reference Ag/AgCl electrode (FLEXREF, World Precision Instruments). The vessel was vigorously purged with argon and irradiated with the full light of an HBO 200 mercury high-pressure lamp. The solution was titrated with a solution of Na_2CO_3 (0.1 M) by using a computer-controlled Medipan 610 B.S infusion pump (Medipan) equipped with calibrated Hamilton syringes and a custom-built interface. The potential of the platinum electrode was measured with a BM-811 digital multimeter (Brymen).

Calculations

Theoretical modeling was performed with Gaussian 03 Rev. D.01 (Gaussian, Inc.)[83] and ArgusLab 4.0.1 (Planaria Software).[84] Preliminary geometry optimization was done with a molecular-mechanics module[85–88] by using the universal force field (UFF),[89–92] and the final geometry was obtained by using DFT with the B3PW91 functional and the 6–311++G(d,p) basis set. Atomic charges were computed with NPO analysis. Molecular orbitals and surfaces were computed by using the same level of theory and tight convergence criteria. Electronic transitions were calculated by using time-dependent DFT with the B3PW91 functional and the 6–311++G(d,p) basis set. Molecular orbitals and charge-distribution diagrams were plotted from Gaussian cube files with the ArgusLab 4.0.1 software.

Acknowledgements

We thank Prof. Janusz Szklarzewicz and Dr. Dariusz Matoga for help with diffuse reflectance measurements, Dr. Wojciech Macyk for valuable discussions, and Mr. Radim Beranek for assistance in the preparation of the manuscript. This work was supported by the Polish Ministry of Education and Science (grants No. PB0941/T08/2005/28, PB1283/T09/2005/29, and PBZ-KBN-118/T09/8). DFT calculations were performed at the Academic Computer Center CYFRONET AGH under computational grant No. MNiI/SGI ONYX/UJ/031/2005.

[1] M. Bendikov, F. Wudl, D. F. Perepichka, *Chem. Rev.* **2004**, *104*, 4891–4945.
[2] J. C. Ellenbogen, J. C. Love, *Proc. IEEE* **2000**, *88*, 386–426.
[3] R. M. Metzger, *Acc. Chem. Res.* **1999**, *32*, 950–957.
[4] H. Meier, *Angew. Chem.* **2005**, *117*, 2536–2561; *Angew. Chem. Int. Ed.* **2005**, *44*, 2482–2506.
[5] R. M. Metzger, *Coll. Surf. A* **2006**, 284–285, 2–10.
[6] D. M. Guldi, G. M. A. Rahman, V. Sgobba, C. Ehli, *Chem. Soc. Rev.* **2006**, *35*, 471–487.
[7] S. Saha, E. Johansson, A. H. Flood, H.-R. Tseng, J. I. Zink, J. F. Stoddart, *Chem. Eur. J.* **2005**, *11*, 6846–6858.
[8] J.-L. Brédas, D. Beljonne, V. Coropceanu, J. Cornil, *Chem. Rev.* **2004**, *104*, 4971–5003.
[9] A. Aviram, M. A. Ratner, *Chem. Phys. Lett.* **1974**, *29*, 277–283.
[10] R. M. Metzger, B. Chen, U. Höpfner, M. V. Lakshmikantham, D. Vuillaume, T. Kawai, X. Wu, H. Tachibana, T. V. Hughes, H. Sakurai, J. W. Baldwin, C. Hosch, M. P. Cava, L. Brehmer, G. J. Ashwell, *J. Am. Chem. Soc.* **1997**, *119*, 10445–10466.
[11] D. Gust, T. A. Moore, A. L. Moore, *J. Photochem. Photobiol. B* **2000**, *58*, 63–71.
[12] D.-L. Jiang, T. Aida, *Prog. Polym. Sci.* **2005**, *30*, 403–422.
[13] H. Imahori, *Org. Biomol. Chem.* **2004**, *2*, 1425–1433.
[14] H. Imahori, Y. Mori, Y. Matano, *J. Photochem. Photobiol. C* **2003**, *4*, 51–83.

[15] N. Martin, L. Sánchez, B. Illescas, I. Pérez, *Chem. Rev.* **1998**, *98*, 2527–2547.
[16] J.-C. Chambron, J.-P. Collin, J.-O. Dalbavie, C. O. Dietrich-Buchecker, V. Heitz, F. Odobel, N. Solladié, J.-P. Sauvage, *Coord. Chem. Rev.* **1998**, *178–180*, 1299–1312.
[17] T. Akiyama, H. Imahori, A. Ajavakom, Y. Sakata, *Chem. Lett.* **1996**, 907.
[18] H. Imahori, H. Norieda, H. Yamada, Y. Nishimura, I. Yamazaki, Y. Sakata, S. Fukuzumi, *J. Am. Chem. Soc.* **2001**, *123*, 100–110.
[19] *Organic Photovoltaics: Concepts and Realization* (Eds: C. J. Brabec, V. Dyakonov, J. Parisi, N. S. Sariciftci), Springer Verlag, Berlin, **2003**.
[20] K. Szaciłowski, W. Macyk, A. Drzewiecka-Matuszek, M. Brindell, G. Stochel, *Chem. Rev.* **2005**, *105*, 2647–2694.
[21] A. Hagfeldt, M. Grätzel, *Acc. Chem. Res.* **2000**, *33*, 269–277.
[22] H. Tributsch, *Coord. Chem. Rev.* **2004**, *248*, 1511–1530.
[23] W. J. E. Beek, M. M. Wienk, R. A. J. Janssen, *J. Mater. Chem.* **2005**, *15*, 2985–2988.
[24] O. Carp, C. L. Huisman, A. Reller, *Progr. Solid State Chem.* **2004**, *32*, 33–177.
[25] M. Biancardo, C. Bignozzi, H. Doyle, G. Redmond, *Chem. Commun.* **2005**, 3918–3920.
[26] L. F. O. Furtado, A. D. P. Alexiou, L. Gonçalves, H. E. Toma, K. Araki, *Angew. Chem.* **2006**, *118*, 3215–3218; *Angew. Chem. Int. Ed.* **2006**, *45*, 3143–3146.
[27] G. Will, J. Sotomayor, S. N. Rao, D. Fitzmaurice, *J. Mater. Chem.* **1999**, *9*, 2297–2299.
[28] K. Szaciłowski, W. Macyk, *Comp. Rend. Chimie* **2006**, *9*, 315–324.
[29] K. Szaciłowski, W. Macyk, G. Stochel, *J. Am. Chem. Soc.* **2006**, *128*, 4550–4551.
[30] K. Szaciłowski, W. Macyk, *Solid State Electron.* **2006**, *50*, 1649–1655.
[31] K. Kalyanasundaram, M. Grätzel, *Coord. Chem. Rev.* **1998**, *177*, 347–414.
[32] A. Hagfeldt, M. Grätzel, *Chem. Rev.* **1995**, *95*, 49–63.
[33] C. A. Mirkin, *Inorg. Chem.* **2000**, *39*, 2258–2272.
[34] C. M. Niemeyer, *Angew. Chem.* **2001**, *113*, 4254–4287; *Angew. Chem. Int. Ed.* **2001**, *40*, 4128–4158.
[35] E. Katz, I. Willner, *Angew. Chem.* **2004**, *116*, 6166–6235; *Angew. Chem. Int. Ed.* **2004**, *43*, 6042–6108.
[36] M.-C. Daniel, D. Astruc, *Chem. Rev.* **2004**, *104*, 293–346.
[37] E. Katz, I. Willner, J. Wang, *Electroanalysis* **2004**, *16*, 19–44.
[38] I. L. Medintz, A. R. Clapp, H. Mattoissi, E. R. Goldman, B. Fisher, J. M. Mauro, *Nat. Mater.* **2003**, *2*, 630–638.
[39] P. Alivisator, *Nat. Biotechnol.* **2004**, *22*, 47–52.
[40] Y. Amao, Y. Yamada, K. Aoki, *J. Photochem. Photobiol. A* **2004**, *164*, 47–51.
[41] K. Tennakone, G. R. R. A. Kumara, K. G. U. Wijayantha, I. R. M. Kottegoda, V. P. S. Perera, G. M. L. P. Aponsu, *J. Photochem. Photobiol. A* **1997**, *108*, 175–177.
[42] J. E. Kroeze, R. B. M. Koehorst, T. J. Savenije, *Adv. Funct. Mater.* **2004**, *14*, 992–998.
[43] J. H. Yu, J. R. Chen, X. S. Wang, B. W. Zhang, Y. Cao, *Chem. Commun.* **2003**, 1856–1857.
[44] A. F. Nogueira, A. L. B. Formiga, H. Winnischofer, M. Nakamura, F. M. Engelmann, K. Araki, H. E. Toma, *Photochem. Photobiol. Sci.* **2004**, *3*, 56–62.
[45] A. F. Nogueira, L. F. O. Furtado, A. L. B. Formiga, M. Nakamura, K. Araki, H. E. Toma, *Inorg. Chem.* **2004**, *43*, 396–398.
[46] H. Winnischofer, A. L. B. Formiga, M. Nakamura, H. E. Toma, K. Araki, A. F. Nogueira, *Photochem. Photobiol. Sci.* **2005**, *4*, 359–366.
[47] C. Ingrosso, A. Petrella, M. L. Curri, M. Striccoli, P. Cosma, P. D. Cozzoli, A. Agostiano, *Appl. Surf. Sci.* **2005**, *246*, 367–371.
[48] J. Pan, G. Benkö, Y. Xu, T. Pascher, L. Sun, V. Sundström, T. Polívka, *J. Am. Chem. Soc.* **2002**, *124*, 13949–13957.
[49] R. Argazzi, N. Y. M. Iha, H. Zabri, F. Odobel, C. A. Bignozzi, *Coord. Chem. Rev.* **2004**, *248*, 1299–1316.
[50] A. S. Polo, M. K. Itokazu, N. Y. M. Iha, *Coord. Chem. Rev.* **2004**, *248*, 1343–1361.
[51] C. G. Garcia, A. S. Polo, N. Y. M. Iha, *J. Photochem. Photobiol. A* **2003**, *160*, 87–91.
[52] F. G. Gao, A. J. Bard, L. D. Kispert, *J. Photochem. Photobiol. A* **2000**, *130*, 49–56.
[53] M. S. Kritsky, T. A. Telegina, T. A. Lyudnikova, A. V. Umrikhina, Y. L. Zemskova, *Dokl. Biochem. Biophys.* **2001**, *380*, 336–338.
[54] P. N. Moorthy, E. Hayon, *J. Org. Chem.* **1977**, *42*, 879–885.
[55] C. Lorente, A. H. Thomas, *Acc. Chem. Res.* **2006**, *39*, 395–402.
[56] T. J. Kappock, J. P. Caradonna, *Chem. Rev.* **1996**, *96*, 2659–2756.
[57] S. Weber, *Biochim. Biophys. Acta* **2005**, *1707*, 1–23.
[58] A. H. Thomas, C. Lorente, A. L. Capparelli, M. R. Pokhrel, A. M. Braun, E. Oliveros, *Photochem. Photobiol. Sci.* **2002**, *1*, 421–426.
[59] U. Diebold, *Surf. Sci. Rep.* **2003**, *48*, 53–229.
[60] F. Seker, K. Meeker, T. F. Kuech, A. B. Ellis, *Chem. Rev.* **2000**, *100*, 2505–2536.
[61] J. F. Endicott in *Comprehensive Coordination Chemistry II*, *Vol. 7* (Eds.: J. A. McCleverty, T. J. Meyer), Elsevier, Amsterdam, **2003**, pp. 657–730.
[62] K. Kanie, M. Nishii, T. Yasuda, T. Taki, S. Ujiie, T. Kato, *J. Mater. Chem.* **2001**, *11*, 2875–2886.
[63] F. Ciuchi, G. Di Nicola, H. Franz, G. Gottarelli, P. Mariani, M. G. Ponzi Bossi, G. P. Spada, *J. Am. Chem. Soc.* **1994**, *116*, 7064–7071.
[64] N. Sakai, Y. Kamikawa, M. Nishii, T. Matsuoka, T. Kato, S. Matile, *J. Am. Chem. Soc.* **2006**, *128*, 2218–2219.
[65] D. Mastropaolo, A. Camerman, N. Camerman, *Science* **1980**, *210*, 333–335.
[66] T. Kato, N. Mizoshita, *Curr. Opin. Solid State Mater. Sci.* **2002**, *6*, 579–589.
[67] L. G. C. Rego, V. S. Batista, *J. Am. Chem. Soc.* **2003**, *125*, 7989–7997.
[68] D. Duonghong, J. Ramsden, M. Grätzel, *J. Am. Chem. Soc.* **1982**, *104*, 2977–2985.
[69] A. M. Roy, G. C. De, N. Sasmal, S. S. Bhattacharyya, *Int. J. Hydrogen Energy* **1995**, *20*, 627–630.
[70] W. Macyk, G. Burgeth, H. Kisch, *Photochem. Photobiol. Sci.* **2003**, *2*, 322–328.
[71] H. Kisch, G. Burgeth, W. Macyk, *Adv. Inorg. Chem.* **2004**, *56*, 241.
[72] K. Szaciłowski, W. Macyk, G. Stochel, *J. Mater. Chem.* **2006**, *16*, 4603–4611.
[73] M. Hebda, G. Stochel, K. Szaciłowski, W. Macyk, *J. Phys. Chem. B* **2006**, *110*, 15275–15283.
[74] K. Szaciłowski, W. Macyk, M. Hebda, G. Stochel, *ChemPhysChem* **2006**, *7*, 2384–2391.
[75] T. J. Meyer, *Pure Appl. Chem.* **1990**, *62*, 1003–1009.
[76] C. R. Bock, J. A. Connor, A. R. Gutierez, T. J. Meyer, D. G. Nagle, *J. Am. Chem. Soc.* **1979**, *101*, 4815–4824.
[77] M. Julliard, M. Chanon, *Chem. Rev.* **1983**, *83*, 425–506.
[78] C. C. Yang, K. C. Hwang, *J. Am. Chem. Soc.* **1996**, *118*, 4693–4698.
[79] D. M. Stanbury, *Adv. Inorg. Chem.* **1989**, *33*, 69–138.
[80] T. Lindgren, J. Lu, A. Hoel, C. C. Grandqvist, G. R. Torres, S.-E. Lindquist, *Solar Energ. Mater. Solar Cells* **2004**, *84*, 145–157.
[81] A. Tsujiko, H. Itoh, T. Kisumi, A. Shiga, K. Murakoshi, Y. Nakato, *J. Phys. Chem. B* **2002**, *106*, 5878–5885.
[82] A. Jańczyk, E. Krakowska, G. Stochel, W. Macyk, *J. Am. Chem. Soc.* **2006**, *128*, 15574–15575.
[83] M. J. Frisch, G. W. Trucks, H. B. Schlegel, G. E. Scuseria, M. A. Robb, J. R. Cheeseman, J. J. A. Montgomery, T. Vreven, K. N. Kudin, J. C. Burant, J. M. Millam, S. S. Iyengar, J. Tomasi, V. Barone, B. Mennucci, M. Cossi, G. Scalmani, N. Rega, G. A. Petersson, H. Nakatsuji, M. Hada, M. Ehara, K. Toyota, R. Fukuda, J. Hasegawa, M. Ishida, T. Nakajima, Y. Honda, O. Kitao, H. Nakai, M. Klene, X. Li, J. E. Knox, H. P. Hratchian, J. B. Cross, V. Bakken, C. Adamo, J. Jaramillo, R. Gomperts, R. E. Stratmann, O. Yazyev, A. J. Austin, R. Cammi, C. Pomelli, J. W. Ochterski, P. Y. Ayala, K. Morokuma, G. A. Voth, P. Salvador, J. J. Dannenberg, V. G. Zakrzewski, S. Dapprich, A. D. Daniels, M. C. Strain, O. Farkas, D. K. Malick, A. D. Rabuck, K. Raghavachari, J. B. Foresman, J. V. Ortiz, Q. Cui, A. G. Baboul, S. Clifford, J. Cioslowski, B. B. Stefanov, G. Liu, A. Liashenko, P. Piskorz, I. Komaromi, R. L. Martin, D. J. Fox, T. Keith, M. A. Al-Laham, C. Y. Peng, A. Nanayakkara, M. Challacombe, P. M. W. Gill, B. Johnson, W. Chen, M. W. Wong, C. Gonza-

lez, J. A. Pople, Gaussian 03 (Rev. D.01), Gaussian, Inc., Wallingford, CT (USA), **2004**.
[84] M. A. Thompson, ArgusLab 4.0, Planaria Software LLC, Seattle, WA (USA), to be found under http://www.arguslab.com, **2004**.
[85] M. A. Thompson, M. C. Zerner, *J. Am. Chem. Soc.* **1991**, *113*, 8210–8215.
[86] M. A. Thompson, E. D. Glendening, D. Feller, *J. Phys. Chem.* **1994**, *98*, 10465–10476.
[87] M. A. Thompson, G. K. Schenter, *J. Phys. Chem.* **1995**, *99*, 6374–6386.
[88] M. A. Thompson, *J. Phys. Chem.* **1996**, *100*, 14492–14507.
[89] C. J. Casewit, K. S. Colwell, A. K. Rappe, *J. Am. Chem. Soc.* **1992**, *114*, 10035–10046.
[90] C. J. Casewit, K. S. Colwell, A. K. Rappe, *J. Am. Chem. Soc.* **1992**, *114*, 10046–10053.
[91] A. K. Rappe, W. A. Goddard, *J. Phys. Chem.* **1991**, *95*, 3358–3363.
[92] A. K. Rappe, K. S. Colwell, C. J. Casewit, *Inorg. Chem.* **1993**, *32*, 3438–3450.

Received: January 29, 2007
Published online: April 10, 2007

